



# Precise radiocarbon determination in radioactive waste by a laser-based spectroscopic technique

Maria Giulia Delli Santi<sup>1a,b</sup>, Giacomo Inero<sup>b,c,d,1,2</sup>, Saverio Bartalini<sup>b,d,e</sup>, Pablo Cancio<sup>b,d,e</sup>, Federico Carcione<sup>e,f</sup>, Iacopo Galli<sup>b,d,e</sup>, Giovanni Giusfredi<sup>b,e</sup>, Davide Mazzotti<sup>b,d,e</sup>, Antonio Bulgheroni<sup>g</sup>, Ana Isabel Martinez Ferri<sup>h</sup>, Rafael Alvarez-Sarandes<sup>g</sup>, Laura Aldave de Las Heras<sup>g</sup>, Vincenzo Rondinella<sup>g</sup>, and Paolo De Natale<sup>d,h</sup>

Edited by David Clark, Los Alamos National Laboratory, Los Alamos, NM; received December 9, 2021; accepted May 9, 2022 by Editorial Board Member Zachary Fisk

The precise and accurate determination of the radionuclide inventory in radioactive waste streams, including those generated during nuclear decommissioning, is a key aspect in establishing the best-suited nuclear waste management and disposal options. Radiocarbon ( $^{14}\text{C}$ ) is playing a crucial role in this scenario because it is one of the so-called difficult to measure isotopes; currently,  $^{14}\text{C}$  analysis requires complex systems, such as accelerator mass spectrometry (AMS) or liquid scintillation counting (LSC). AMS has an outstanding limit of detection, but only a few facilities are available worldwide; LSC, which can have similar performance, is more widespread, but sample preparation can be nontrivial. In this paper, we demonstrate that the laser-based saturated-absorption cavity ring-down (SCAR) spectroscopic technique has several distinct advantages and represents a mature and accurate alternative for  $^{14}\text{C}$  content determination in nuclear waste. As a proof-of-principle experiment, we show consistent results of AMS and SCAR for samples of concrete and graphite originating from nuclear installations. In particular, we determined mole fractions of 1.312(9)  $\text{F}^{14}\text{C}$  and 30.951(7)  $\text{F}^{14}\text{C}$  corresponding to  $\sim 1.5$  and 36.2 parts per trillion (ppt), respectively, for two different graphite samples originating from different regions of the Adiabatic Resonance Crossing activator prototype installed on one irradiation line of an MC40 Scanditronix cyclotron. Moreover, we measure a mole fraction of 0.593(8)  $\text{F}^{14}\text{C}$  ( $\sim 0.7$  ppt) from a concrete sample originating from an external wall of the Ispra-1 nuclear research reactor currently in the decommissioning phase.

nuclear waste | decommissioning | radiocarbon | nuclear safety | saturated-absorption cavity ring-down spectroscopy

The management and disposal of radioactive waste from nuclear technologies operations and decommissioning require accurate radionuclides inventories; most of the relevant species are in sufficient concentration or are suited to be detected and measured by rather conventional techniques, in particular gamma spectroscopy. However, there is a group of key nuclides that are important for radiological assessment of waste but have a significantly low abundance and/or a decay fingerprint not well suited for radiometric analysis. This group of difficult to measure (DTM) species includes  $^{14}\text{C}$ ,  $^{36}\text{Cl}$ ,  $^{90}\text{Sr}$ ,  $^{107}\text{Pd}$ , and other pure alpha and beta emitters, often with half-lives of several thousand years and a low penetrating power of the emitted radiation. For some of them (e.g., the fission product  $^{90}\text{Sr}$ ), the production route (by neutron irradiation of the fuel in the nuclear reactor) is well defined, and consequently, its quantification by means of the isotopic vector technique is sufficiently reliable. For others, such as  $^{14}\text{C}$ , this approach is not applicable because of the complex production route(s), which makes its estimation by calculations very difficult, essentially leaving its direct determination by analytical techniques the only suitable alternative. Some of these DTM isotopes ( $^{14}\text{C}$  and  $^{36}\text{Cl}$ ) belong to the family of the so-called dose-relevant nuclides. Indeed, as a consequence of their chemistry, mobility, and interaction with biogeochemical cycles, in case of uncontrolled release they would have a high radiological impact in terms of dose delivered to humans and to the biosphere (1).

This research paper aims to demonstrate that a class of laser-based spectrometers is now a mature technology able to address the issue of accurate determination of  $^{14}\text{C}$  content in materials originating from nuclear power plants (NPPs). Accelerator mass spectrometry (AMS) is the gold standard for low-abundance rare isotopes quantification with an outstanding limit of detection, but its availability is limited to a few instruments in developed countries. On the other hand, liquid scintillation counting (LSC) can provide adequate analytical performance for many applications at a more reasonable cost and with a much wider availability; nevertheless, the sample preparation often requires laborious elemental separations. While a comparison among the performances of the three

## Significance

Radiocarbon ( $^{14}\text{C}$ ) is a naturally occurring long-lived radioactive isotope whose secular equilibrium is governed by cosmic rays interaction. It is also artificially generated in nuclear reactors and irradiation facilities, posing a risk to living organisms if not properly confined. The amount of  $^{14}\text{C}$  in the nuclear waste streams is difficult to quantify utilizing established techniques. This paper shows that saturated-absorption cavity ring-down (SCAR), a laser-based technique, can be profitably used in the analysis of low  $^{14}\text{C}$  concentrations present in materials such as graphite and concrete, which are representative of large volumes of nuclear decommissioning waste. We show that SCAR provides excellent analytical performance when the sample is correctly prepared, reducing any spectral interference down to a negligible level.

Competing interest statement: S.B., P.C., I.G., G.G., D.M., and P.D.N. are founding partners of ppqSense S.r.l.

This article is a PNAS Direct Submission. D.C. is a guest editor invited by the Editorial Board.

Copyright © 2022 the Author(s). Published by PNAS. This article is distributed under [Creative Commons Attribution-NonCommercial-NoDerivatives License 4.0 \(CC BY-NC-ND\)](https://creativecommons.org/licenses/by-nc-nd/4.0/).

<sup>1</sup>M.G.D.S. and G.I. contributed equally to this work.

<sup>2</sup>To whom correspondence may be addressed. Email: giacomo.inero@ino.cnr.it.

This article contains supporting information online at <https://www.pnas.org/lookup/suppl/doi:10.1073/pnas.2122122119/-DCSupplemental>.

Published July 7, 2022.

techniques (AMS, LSC, and saturated-absorption cavity ring-down [SCAR]) is outlined, in this paper SCAR results were validated only against AMS.

## Radiocarbon in NPPs

Before the 1960s, the atmospheric concentration of  $^{14}\text{C}$  was almost stable and governed by its natural production by cosmic ray interactions in the upper troposphere and stratosphere. After that date, additional  $^{14}\text{C}$  was introduced in the atmosphere, with nuclear weapons and NPPs as the two main anthropogenic sources (2). In nuclear reactors,  $^{14}\text{C}$  is mainly produced by neutron-induced nuclear reactions involving some specific isotopes of nitrogen, oxygen, and carbon. Table 1 lists the three main reaction pathways along with the natural abundance of the target isotope and the reaction cross-section for thermal neutrons (25 meV). Other neutron-induced reactions having  $^{14}\text{C}$  as final product exist [such as  $^{15}\text{N}(n, d)^{14}\text{C}$ ,  $^{16}\text{O}(n, 2pn)^{14}\text{C}$ , and  $^{18}\text{O}(n, n\alpha)^{14}\text{C}$ ], but they are negligible because of the extremely low cross-section in the thermal neutron energy range.

Nitrogen, oxygen, and carbon are present in every region of a nuclear reactor exposed to the neutron flux, but their concentration levels can vary significantly, resulting in a very complex determination of the main  $^{14}\text{C}$  production route. For example, the main production routes taking place in graphite moderators present in advanced gas-cooled reactors are based on both  $^{13}\text{C}$  and  $^{14}\text{N}$  isotopes. Despite the abundance of carbon, the higher cross-section of the  $(n, p)$  reaction on  $^{14}\text{N}$  makes the nitrogen-mediated reaction significant. In fact, air bubbles are trapped in graphite porosity and bombarded by a neutron flux of  $10^{14} \text{ cm}^{-2} \text{ s}^{-1}$  in the reactor core. Another example is the cooling water used in the great majority of operating NPPs, where the water-dissolved nitrogen represents the main production route for  $^{14}\text{C}$ . The radioactive element is partially trapped on the cooling water purification resins, which represent an important source of  $^{14}\text{C}$  in nuclear waste (5), and it is partially released in the form of  $\text{CO}_2$  or  $\text{CH}_4$  from the plant stack, possibly along with other volatile fission products, like Xe isotopes (6). While it is relatively easy to monitor and quantify Xe emission, online measurements of  $^{14}\text{C}$  are still a challenging task currently under development (7).

Structural materials, like steel and concrete, can also contain traces of the target isotopes either incorporated during production or present in the superficial layer, and thus, when exposed to a neutron flux, they contribute to the  $^{14}\text{C}$  inventory. Since the amount of target isotopes in the structural material is provided by the producers as upper limits or with too high uncertainties, an a priori estimation of the final  $^{14}\text{C}$  inventory is unreliable.

Notwithstanding the fact that the activity of  $^{14}\text{C}$  in nuclear waste is very small when compared with other radionuclides, if we consider the hypothetical total dose as resulting from the release of all radionuclides from low-/intermediate-level waste (LILW) disposal facilities and NPP operations, a dominant contribution is generally associated with  $^{14}\text{C}$  (8, 9). This is primarily connected to

**Table 1. The three neutron-induced nuclear reactions that mainly contribute to the  $^{14}\text{C}$  production in NPPs**

Reaction	Natural abundance, %	Cross-section, mbarn
$^{14}\text{N}(n, p)^{14}\text{C}$	99.64	1,868 (3)
$^{17}\text{O}(n, \alpha)^{14}\text{C}$	0.038	249 (3)
$^{13}\text{C}(n, \gamma)^{14}\text{C}$	1.07	1.5 (4)

For each reaction, the target isotope natural abundance and reaction cross-section for thermal neutrons (25 meV) are reported.

the chemistry of the radiocarbon-bearing molecular species;  $\text{CO}_2$  and  $\text{CH}_4$  are volatile and nonreactive, so they can migrate from the storing and production sites and be taken up in the biological life cycle.

This work focuses on the development of a rapid and simple technique for measuring the  $^{14}\text{C}$  concentration in nuclear waste, which is necessary for the characterization and classification of the waste and the selection of an appropriate waste disposal option and its assessment. In fact, the engineered barrier system of the waste repository must be designed in a way to contain both inorganic and organic  $^{14}\text{C}$ -bearing molecules that would otherwise be taken up by plants and reach human beings. A precise and accurate knowledge of  $^{14}\text{C}$  concentration can dictate the choice of the best-fitting waste form and disposal method, such as shallow or deep repository. The major interest of  $^{14}\text{C}$  analysis is focused on the LILW streams. As stressed by International Atomic Energy Agency (IAEA) (10), it is necessary to control the  $^{14}\text{C}$  production at nuclear facilities but also, to have proper management of the related waste.  $^{14}\text{C}$  can be the inventory-limiting nuclide at LILW disposal facilities. This may be the case for one of the two major US LILW disposal sites, where the relatively high  $^{14}\text{C}$  inventory may cause an early closing of the repository before reaching its full volumetric filling capacity (11).

Reliable determination of  $^{14}\text{C}$  in nuclear waste can effectively address the problems expressed above, but so far, the technical difficulties associated with experimental measurement have resulted in methods that are not precise or sensitive enough. The most common approach to establish the total  $^{14}\text{C}$  content of a waste package is the usage of scaling factors (12) defined as the ratio between a DTM isotope and one or more specific easy to measure radionuclides. In the case of  $^{14}\text{C}$ , it is assumed that its concentration is directly related to that of  $^{60}\text{Co}$  via a scaling factor derived through both experimental and theoretical analyses. Unfortunately, the scaling factor of  $^{60}\text{Co}$  cannot be used for all waste types [for example, it is not applicable for the ion-exchange resins (13)]. A different approach relies on the calculation of  $^{14}\text{C}$  content derived from the nitrogen impurities concentration. This process assumes an exact knowledge of the production mechanism, impurities concentrations, and neutron irradiation history. Both of these methods are affected by large uncertainties and often provide incompatible results, like in the case of the Swedish final repository for short-lived radioactive waste, where different models resulted in  $^{14}\text{C}$  estimations with a factor of 2.6 discrepancy (14). The current estimation models based on scaling factors and activation rates of the precursors would, therefore, strongly benefit from or in some cases, even be overtaken by an easily accessible and affordable quantification based on experimental campaigns as also shown within the framework of the CARbon-14 Source Term (CAST) project (15).

The direct measurement approach mainly relies on AMS and LSC. AMS can reach a limit of detection as low as  $0.002 \text{ F}^{14}\text{C}^*$  for a typical 0.1– to 1-mg C sample (18). Concerning precision, AMS and LSC perform similarly, but LSC requires a few grams of C to be dissolved in the scintillation mixture (19).

Laser-based spectroscopic methods have also been demonstrated for this task. While linear-absorption cavity ring-down spectroscopy (CRD) achieved, in the best case, a precision of 0.11  $\text{F}^{14}\text{C}$  (20, 21), SCAR demonstrated a precision of  $0.004 \text{ F}^{14}\text{C}$

\*One  $\text{F}^{14}\text{C}$ , or modern, corresponds to the  $^{14}\text{C}$  mole fraction in a natural C sample collected in 1950 before the nuclear bomb testing suddenly changed the concentration equilibrium in the atmosphere (doubling it in only a few years), having a specific activity of 0.226 Bq/g. Combining this value with the half-life of 5,700(30) y (16), the obtained modern mole fraction is 1.169(6) ppt. Other practical units of measurement for  $^{14}\text{C}$  content are described in ref. 17.

(22), proving to be nowadays the single most reliable competitor of AMS in terms of precision, making use of a few milligrams of C material with a much more compact and smaller footprint instrument.

A system similar to the one presented in ref. 22 has been built up in an inactive laboratory of the Joint Research Centre (JRC) Karlsruhe. As soon as the optical setup commissioning is accomplished and its performance is assessed against reference standards, it will be moved to the controlled area and coupled to a carbon extraction system operating in a radiation-controlled environment. In this way, it will be possible to assess the  $^{14}\text{C}$  content of highly radioactive and contaminated samples, such as reactor vessel structural material, the fuel cladding, and also, the nuclear fuel itself. In fact, the JRC is equipped with unique infrastructures, including heavily shielded hot cells with telemanipulators and airtight gloveboxes, to safely handle radioactive materials. The SCAR setup will allow us to determine the  $^{14}\text{C}$  content from nuclear applications with unprecedented precision. In this paper, we show a proof-of-principle application of SCAR technology to nuclear waste of different radioactivity levels by measuring the  $^{14}\text{C}$  concentration in two graphite samples and one concrete sample and comparing the obtained results with AMS independent measurements. The concrete sample is a relevant example of a relatively large volume of decommissioning material with mainly modern or submodern expected  $^{14}\text{C}$  content. Should the measured  $^{14}\text{C}$  and other artificial radionuclides be below the clearance exemption limit ( $1\text{ Bq g}^{-1}$  for  $^{14}\text{C}$ ; i.e., about  $4\text{ F}^{14}\text{C}$ ) (23), the concrete could be cleared and disposed of as conventional waste, not going through nuclear waste repositories. Considering the big volume of concrete, this would result in a remarkable economic impact on the overall investment for decommissioning. The irradiated graphite is another interesting sample since its activity can span up to hundreds of  $\text{kBq g}^{-1}$  (24). As such, it demonstrates the capability of SCAR to measure samples in an enrichment range inaccessible to AMS without dilution.

## Materials and Methods

**Sample Origin and Preparation.** Both graphite and concrete samples were collected at the European Commission JRC site located in Ispra (Italy) from two different nuclear installations currently under decommissioning. The concrete sample (identified as KB in the following sections) came from the external wall of the Ispra-1 nuclear reactor (25). This was a 5-MW Chicago-Pile-type reactor built in northern Italy in 1957 to become the first nuclear reactor in Italy to reach criticality. In its early stage of operation, its title was transferred to the European Community of Atomic Energy, and then, it was operated under the European Atomic Energy Community (EURATOM) treaty by the JRC. It provided an intense neutrons beam for condensed matter investigations, valuable experimental results in the field of core physics, radiation-tolerant material science, and neutron interaction with living matter.

The graphite material originated from the Adiabatic Resonance Crossing activator prototype (26) installed on one irradiation line of an MC40 Scanditronix cyclotron. Along this beamline, protons were accelerated to a kinetic energy of at least 36 MeV before colliding against a thick beryllium target. By interaction with the target material, a large flux of fast neutrons was produced and thermalized by a cubic meter reflector made of nuclear-grade graphite. The whole-neutron energy spectrum (from several megaelectronvolts down to the thermal range) was confined in the graphite volume and forced to cross the region of the activation channels where samples were loaded. The graphite reflector was made by several graphite bricks whose activation levels vary significantly from one another due to their position. Two samples were taken from different bricks, and they are identified as KG1 and KG2 in the following sections.

Both sample types were ball milled with agate spheres in order to obtain a fine powder. Since the concrete sample was obviously heterogeneous, an additional sieving step was performed; the milling and sieving cycle was repeated until all

the original material was below  $100\ \mu\text{m}$ . Graphite, being homogeneous, was not sieved. All samples were prepared in two replicas of 1 g each: one to be used for AMS measurements and one for SCAR. The total carbon determination of the concrete sample was performed by means of an International Organization for Standardization (ISO)-certified calibrated elemental analyzer and resulted in a carbon mass fraction of  $(3.53 \pm 0.06)\%$ .

**Carbon Extraction and Oxidation.** In order to perform  $^{14}\text{C}$  mole fraction analyses with AMS, the carbon content of the initial sample must be converted to either graphite or  $\text{CO}_2$ . Since SCAR is operating on a gaseous  $\text{CO}_2$  sample, we decided to perform both analyses on gases. Carbon extraction and oxidation were done using dedicated elemental analyzers (EuroVector EA 3000 for AMS and Elementar Vario Isotope Cube for SCAR), where the input material is combusted at high temperature in a pure oxygen atmosphere.<sup>†</sup> The gaseous products are flowed by a carrier gas (He) through a reduction tube and a gas-selective adsorption column that traps  $\text{CO}_2$  until it is heated up. The  $\text{CO}_2$  fraction is separated from the carrier gas and purified from other gases using either a zeolite trap (AMS) or a cryogenic bath (SCAR) before being transferred to the analytical apparatus.

**AMS Measurements.** The  $^{14}\text{C}$  mole fraction determination of the three samples was outsourced to the University of Cologne, where a 6-MV tandemron accelerator system built by High Voltage Engineering Europa B.V. is routinely used for carbon dating and measurements of cosmogenic nuclides. The accelerator system contains two identical ion sources; one is dedicated to the measurement of solid samples, while the other is connected to a gas handling system and dedicated to  $\text{CO}_2$  measurements. The  $^{14}\text{C}/^{12}\text{C}$  declared precisions are 0.35 and 1% for a sample with a 1  $\text{F}^{14}\text{C}$  mole fraction, respectively, for the two ion sources (27). For this work, only the second ion source has been used. For each sample, 10 replicas (10 and 0.1 mg each for concrete and graphite, respectively) were combusted and independently measured after an instrument blank run and a suitable calibration were performed.

Preliminary results obtained with the SCAR method allowed us to determine the  $^{14}\text{C}$  mole fraction range; for KB and KG1, this was found to be around one modern, while KG2 was found in the tens modern range. This preliminary estimation is particularly important for AMS analysis in order to define a dilution strategy, thus avoiding a too heavy contamination of the accelerator in the case of a higher than modern  $^{14}\text{C}$  mole fraction. Following this preliminary analysis, the KG2 sample was diluted in solid forms, adding a precise amount of "fossil" graphite. The analytical balance used for the dilution has a readability of 0.01 mg and a relative 0.1% uncertainty referred to the measured mass of 100 mg. The diluted sample was carefully homogenized and divided in 10 samples, which were burnt individually in the elemental analyzer and transferred to the AMS ion source.

**SCAR Measurements.** The SCAR spectrometer used for these measurements is located at the Consiglio Nazionale delle Ricerche, Istituto Nazionale di Ottica laboratory in Florence. It requires at least 7 mg of carbon in order to achieve its best precision. We obtained such a quantity by burning a single unit of 9 mg of graphite (for both KG1 and KG2 samples) and nine different units of 38 mg each of concrete (KB sample), resulting in a combusted total mass of 342 mg. The highly pure  $\text{CO}_2$  gas was then injected into the SCAR spectrometer. The SCAR experimental setup is already described in refs. 22 and 28. Here, we provide only the most relevant information on the technique. In SCAR spectroscopy, laser light is coupled to a high-finesse two-mirror optical cavity up to a threshold level in the transmitted power, and then, it is quickly switched off. Transmitted light during the ring-down process is detected, and the decay rate is measured. If a molecular species inside the cavity absorbs the coupled light, it increases the cavity loss rate, and such variation is measured. The difference with respect to conventional CRD spectroscopy is that saturation effects on the molecular absorption induce a deviation of the ring-down signal from a perfectly exponential behavior, as expected for linear intracavity losses. Starting from an ab initio theoretical model, a fitting routine was developed taking into account the transient effects due to

<sup>†</sup>EuroVector model EA 3000 runs at a temperature of  $1,020\ ^\circ\text{C}$  with 13-s oxygen flux, while the Elementar mod. Vario Isotope Cube runs at  $900\ ^\circ\text{C}$  with 120 and 210 s of oxygen flux for graphite and concrete, respectively. The different combustion/oxidation durations have no effect on the measurement results. Both instruments are used in mass spectroscopy experiments because they are known not to introduce any isotopic fractionation bias.

a changing saturation level; the routine retrieves from each single CRD decay event both the empty-cavity and the gas-induced losses (22). The  $^{14}\text{C}$  mole fraction is determined by measuring the spectral area of its ( $00^0_1 - 00^0_0$ ) P(20) ro-vibrational transition at  $2,209.1077\text{ cm}^{-1}$ , whose profile is recorded with high spectral fidelity by scanning the cavity frequency. One back-and-forth stepwise scan of the frequency across the target transition is performed for each acquisition. Each scan spans 650 MHz, with 66 points spaced by 10 MHz, and takes about 6 min. For each frequency step, 5,000 SCAR signals are acquired and averaged. Assuming the same effective saturation parameter for the whole frequency scan, the gas-induced cavity decay rate function  $\gamma_g(\nu)$  is determined by averaging together the values belonging to the single sweeps. For each sample, 28 spectra of  $\gamma_g$  across the P(20) line are recorded (for a total measuring time around 3 h) and fitted using a two-line manifold Voigt profile. The fitting function is obtained considering the target line of  $^{14}\text{C}$  and an interfering line of  $\text{N}_2\text{O}$  at  $2,209.0854\text{ cm}^{-1}$  that is, however, strongly suppressed during sample preparation. To obtain an estimate of the  $^{14}\text{C}$  content in each sample, a relative measurement was performed by comparing it with a standard reference material (SRM). Fig. 1A shows the average of 142 measurements of the SRM containing a carbon mass fraction of  $\sim 19\%$  and a  $^{14}\text{C}$  mole fraction of  $1.3407\text{ F}^{14}\text{C}$ . Fig. 1B shows the average of 28 measurements of the KG1 sample. Both measurements were fit to a two-Voigt function, also taking into account the small interfering  $\text{N}_2\text{O}$  peak. Residuals from the fit are shown in Fig. 1A, Lower and B, Lower. The green shaded area represents the fit result for the SRM and is used to calculate the  $^{14}\text{C}$  content in all samples.

## Results and Discussion

The AMS results from all the subsamples analyses were provided by the University of Cologne team. For KG2, the addition of fossil graphite resulted in a dilution factor of 10.977. No dilution was required for the SCAR analyses. In Fig. 2 A–C, we report the complete measurement results for the two graphite (KG1 and KG2) and concrete (KB) samples obtained via AMS and SCAR (SI Appendix, Tables S1 and S2 have data).

With the optical method, we performed 28 repeated measurements for each sample, while a single measurement on 10 different subsamples, for each sample, was performed by AMS. One AMS measurement for KG1 and two measurements for KG2 were excluded from the plot and from the statistical analysis because they were affected by a systematic “memory” effect due to previously measured enriched samples (not part of this work).

The AMS reported uncertainty is, as expected, about 1% for all measurements; this is a consequence of the Poissonian statistics of the ion counting process. The SCAR uncertainty is about  $0.03\text{ F}^{14}\text{C}$  for all measurements; this depends on the signal-to-noise ratio of the raw data and on the acquisition parameters (22). In order to account for systematic effects, the final  $^{14}\text{C}$  content values for KG1, KG2, and KB have been obtained by calculating the weighted average and its uncertainty for both AMS and SCAR measurements. Applying a two-sample  $t$  test for the three sample materials, it is confirmed that for KG1 and KB, the null hypothesis ( $H_0$ : AMS and SCAR provide the same results) is retained with a  $P$  value  $> 0.05 = \alpha$ .

For KG2, the  $t$  test rejected the null hypothesis. Thus, from a statistical point of view, the two techniques are not providing the same results. This conclusion is clear when comparing the AMS and SCAR datasets (Fig. 2B). A trend is evident in the AMS data. Possible inhomogeneity in the original KG2 sample can impact only the AMS results since the measurement is performed on different subsamples. However, the clear decreasing trend of the individual subsamples (Fig. 2B) suggests some kind of systematic error that was not possible to identify. Since the linearity, as a function of the  $^{14}\text{C}$  mole fraction, of the optical method was already demonstrated in the past (29) and since the two techniques provide consistent results for KG1 and KB, we believe that the SCAR result for the KG2 sample is correct, while the AMS one is affected by a systematic error.

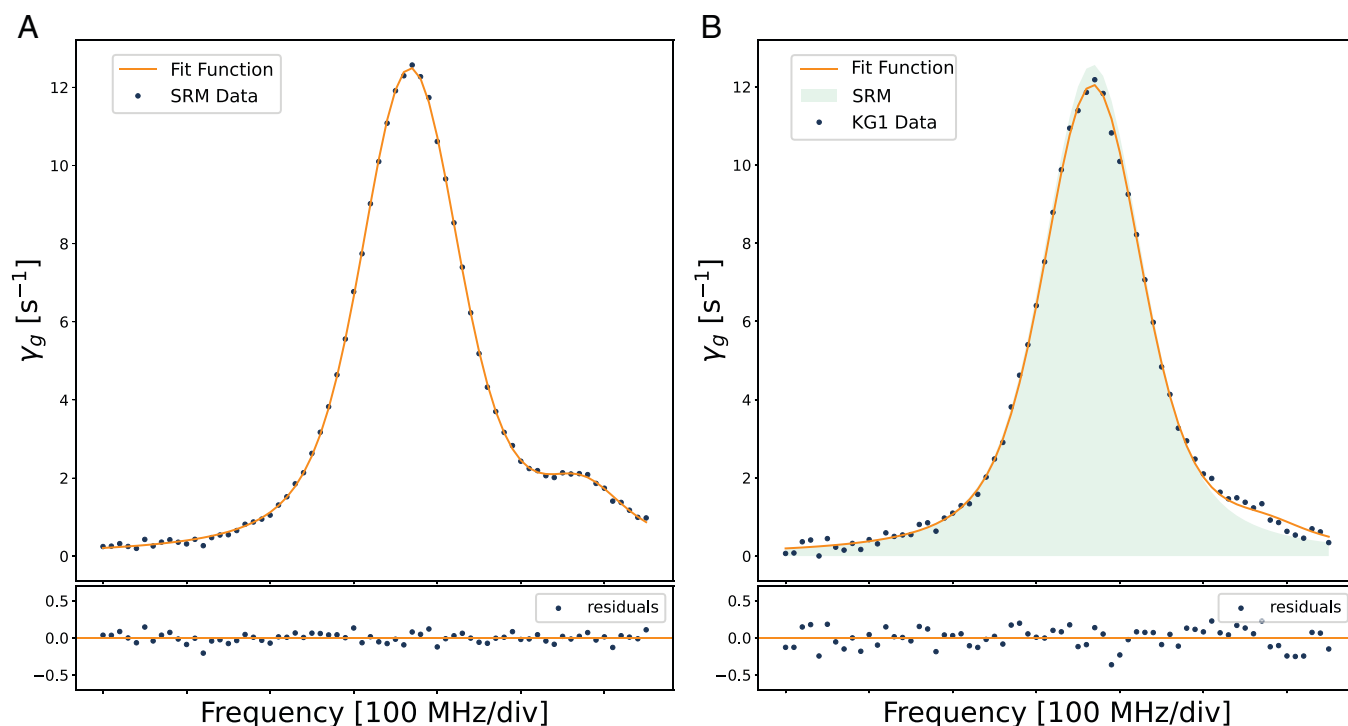


**Fig. 1.** (A) Average spectrum of the P(20) line of  $^{14}\text{C}$  measured for the SRM oxalic acid dihydrate ( $\text{C}_2\text{H}_2\text{O}_4 \cdot 2\text{H}_2\text{O}$ ) provided by the National Institute of Standards and Technology (SRM 4990C) with a carbon mass fraction of  $\sim 19\%$  and a  $^{14}\text{C}$  mole fraction of  $1.3407\text{ F}^{14}\text{C}$ . (B) Average spectrum of the P(20) line of  $^{14}\text{C}$  measured for the KG1 sample with a  $^{14}\text{C}$  mole fraction of  $1.312(9)\text{ F}^{14}\text{C}$ . Both measurements were performed with the SCAR spectrometer, and data were fit to a two-Voigt function, also taking into account the small interfering  $\text{N}_2\text{O}$  peak. Residuals from the fit are shown in A, Lower and B, Lower. The green shaded area represents the fit result for the SRM and is used to calculate the  $^{14}\text{C}$  content in all samples.

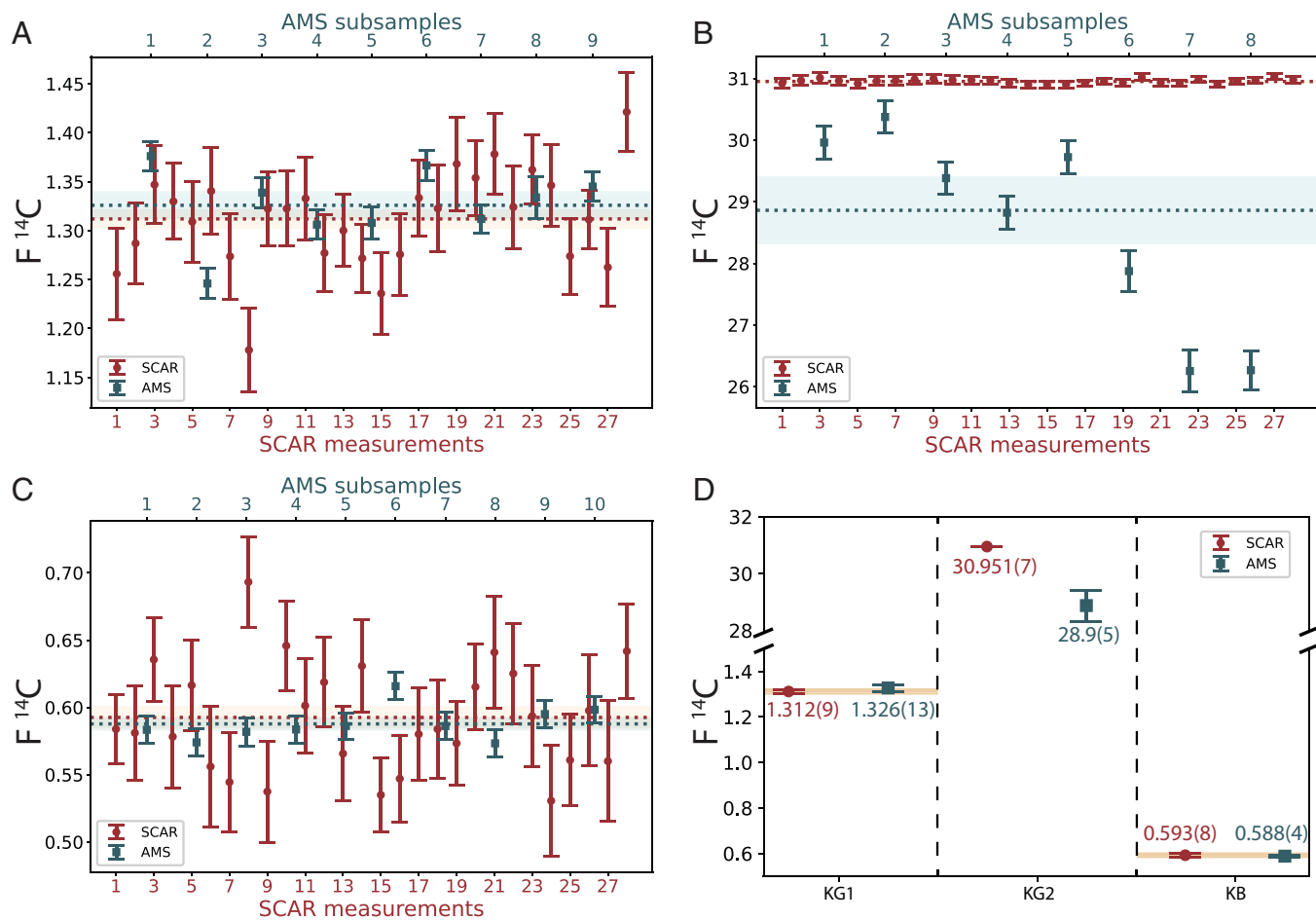


**Fig. 2.** (A) Measurements of the KG1 sample of graphite. (B) Measurements of the KG2 sample of graphite. (C) Measurements of the KB sample of concrete. SCAR results (red circles) refer to the repeated measurements of the same gas sample produced by a single combustion, while AMS points (blue squares) refer to gas samples produced by the combustion of different subsamples. The dotted lines and the shaded areas represent the weighted means and their uncertainties for the two techniques, respectively. (D) Comparison between the weighted means obtained with the two techniques for the three samples. The yellow shaded areas highlight the error bars of the SCAR measurements, except for the KG2 data since the two measurements are not statistically consistent. SCAR and AMS data are reported in *SI Appendix, Tables S1 and S2*, respectively.

For the AMS and SCAR analyses, the graphite is generally powdered via a ball-mill grinder. Depending on the size of the graphite pores, powder granulometry, and gas diffusion in powder grains, the measured fraction of  $^{14}\text{C}$  can be an underestimation of the overall initial  $^{14}\text{C}$  content. Part of gaseous  $^{14}\text{C}$  compounds trapped in material pores can be released during grinding and not measured, providing a lower than real activity. This is a crucial problem that has to be further investigated in further works because it could potentially influence the definition of a waste management option, but it is not affecting the goodness of the analytical technique by itself. A similar situation may also apply to other porous materials like concrete, where one should also consider the heterogeneity of different phases.

## Conclusions

In this work, we have demonstrated that the laser-based SCAR technique is now a mature, accurate, and relatively simple alternative to the well-established AMS and LSC techniques in the determination of  $^{14}\text{C}$  content at mole fraction levels ranging from below modern to enriched. The presented approach is able to provide results for  $^{14}\text{C}$  content in around 5 min after a careful sample combustion has been done avoiding spectroscopic interference from  $\text{N}_2\text{O}$ , paving the way to a class of relatively small footprint instruments able to process many samples at the

place of origin. For nuclear decommissioning, this would have a huge impact since the possibility of on-site measurement avoids the complex, often totally forbidden organization of radioactive transport, strongly reducing unnecessary radiological exposure. In many circumstances, precise determination of the  $^{14}\text{C}$  content in the decommissioning waste will allow for the clearance of large volumes of LILW as conventional waste, not only reducing the overall cost but also, mitigating the environmental impact of nuclear waste management.

Also, LSC can be profitably used for samples with higher specific activities, like KG2, and those requiring dilution for AMS. In ref. 30, the  $\text{CO}_2$  produced by the combustion of irradiated graphite in an elemental analyzer was bubbled in a basic solution and then mixed with the scintillation mixture. A measurement campaign aiming at comparing LSC and SCAR has been foreseen and will be reported in a future paper.

The SCAR technique can be also adapted to measure other nuclear safety-related nuclides, such as  $^{36}\text{Cl}$ , which is another important DTM isotope. Preliminary work on these radionuclide has been conducted by the VTT Technical Research Centre of Finland (31).

A clear advantage of the optical method with respect to the ion-based (AMS) one is the much higher measurement dynamic range. AMS operators are very reluctant to measure enriched samples because of the risk of long-term contamination of the ion



chamber. Furthermore, the necessary dilution can be a potential source of additional uncertainties. Instead, we demonstrate that the SCAR system can measure up to 30 times the modern without any memory effect and without any dilution. The AMS requires ~50 times less mass than the optical system to perform the measurement, making it very sensitive to possible  $^{14}\text{C}$  inhomogeneous distribution over multiphase materials. On the other hand, for applications to nuclear waste, the larger quantities needed by SCAR are not a limitation and can even be beneficial in simplifying the homogenization procedure.

**Data Availability.** Zipped comma-separated values (CSV) and text (TXT) data files have been deposited in the Joint Research Centre Data Catalogue (<https://data.europa.eu/89h/7002ce48-f46a-4d19-be3b-37f93852b586>) (32).

**ACKNOWLEDGMENTS.** We thank Prof. Roberto Caciuffo for his contribution in importing the SCAR technology into the nuclear field. We also thank the team of the CologneAMS at the University of Cologne and in particular, Dr. Erik Strub for

endless support in the interpretation of the AMS results and the Analytical Service of the Joint Research Centre (JRC) Karlsruhe for the total carbon determination. The realization of a SCAR setup in Karlsruhe was funded by the European Commission, Joint Research Centre under the Exploratory Research Programme.

Author affiliations: <sup>a</sup>Consiglio Nazionale delle Ricerche, Istituto Nazionale di Ottica, 80078 Pozzuoli, Italy; <sup>b</sup>Consiglio Nazionale delle Ricerche, Istituto Nazionale di Ottica, 50019 Sesto Fiorentino, Italy; <sup>c</sup>Istituto Nazionale di Ricerca Metrologica, 10135 Torino, Italy; <sup>d</sup>European Laboratory for Non-Linear Spectroscopy, 50019 Sesto Fiorentino, Italy; <sup>e</sup>ppqSense S.r.l., 50013 Campi Bisenzio, Italy; <sup>f</sup>Dipartimento di Ingegneria Industriale, Università degli Studi di Firenze, 50139 Firenze, Italy; <sup>g</sup>European Commission, Joint Research Centre (JRC), 76125 Karlsruhe, Germany; and <sup>h</sup>Consiglio Nazionale delle Ricerche, Istituto Nazionale di Ottica, 50125 Firenze, Italy

Author contributions: G.I., S.B., P.C., I.G., G.G., D.M., A.B., L.A.d.L.H., and P.D.N. designed research; M.G.D.S., G.I., and A.B. performed research; A.I.M.F. contributed new reagents/analytic tools; M.G.D.S., G.I., F.C., A.B., and R.A.-S. analyzed data; A.I.M.F., L.A.d.L.H., and V.R. provided resources to experimental and data processing; M.G.D.S., G.I., A.B., and V.R. wrote the paper; and S.B., P.C., D.M., A.I.M.F., R.A.-S., L.A.d.L.H., V.R., and P.D.N. reviewed the manuscript.

1. W. Hummel, "Chemistry of selected dose-relevant radionuclides" (Tech. Rep. 1015-2636, Paul Scherrer Institute (PSI), Villigen, Switzerland, 2017).
2. H. Xiaolin, Tritium and  $^{14}\text{C}$  in the environment and nuclear facilities: Sources and analytical methods. *J. Nucl. Fuel Cycle Waste Technol.* **16**, 11–39 (2018).
3. R. Kitahara *et al.*, Improved accuracy in the determination of the thermal cross section of  $^{14}\text{N}(n,p)^{14}\text{C}$  for neutron lifetime measurement. *Prog. Theor. Exp. Phys.* **2019**, 093C01 (2019).
4. T. Wright *et al.*, Measurement of the  $^{13}\text{C}(n,\gamma)$  thermal cross section via neutron irradiation and AMS. *Eur. Phys. J. A* **55**, 200 (2019).
5. A. Magnusson, K. Stenström, P. O. Aronsson,  $^{14}\text{C}$  in spent ion-exchange resins and process water from nuclear reactors: A method for quantitative determination of organic and inorganic fractions. *J. Radioanal. Nucl. Chem.* **275**, 261–273 (2008).
6. M. B. Kalinowski, M. P. Tuma, Global radionuclide emission inventory based on nuclear power reactor reports. *J. Environ. Radioact.* **100**, 58–70 (2009).
7. G. Genoud *et al.*, Laser spectroscopy for monitoring of radiocarbon in atmospheric samples. *Anal. Chem.* **91**, 12315–12320 (2019).
8. United Nations Scientific Committee on the Effects of Atomic Radiation (UNSCEAR), "Sources and effects of ionizing radiation, report to the general assembly" (Tech. Rep. No. E.00.IX.3, ISBN 92-1-142238-8, United Nations, New York, NY 2000).
9. S. V. Churakov, W. Hummel, M. M. Fernandes, Fundamental research on radiochemistry of geological nuclear waste disposal. *Chimia (Aarau)* **74**, 1000–1009 (2020).
10. International Atomic Energy Agency, "Management of waste containing tritium and carbon-14" (Tech. Rep. STD/DOC/010/421, IAEA, Vienna, Austria, 2004).
11. M. S. Yim, F. Caron, Life cycle and management of carbon-14 from nuclear power generation. *Prog. Nucl. Energy* **48**, 2–36 (2006).
12. M. Kashiwagi *et al.*, "ISO Standardization of the Scaling Factor Method for Low- and Intermediate Level Radioactive Wastes Generated at Nuclear Power Plants." in *Proceedings of the 11th International Conference on Environmental Remediation and Radioactive Waste Management*. (Bruges, Belgium, September 2–6, 2007), pp. 625–629.
13. G. Buckau, D. Bottomley, E. A. C. Neeft, "(d7.11) CAST project report" (Tech. Rep. D7.11, Project CAST, European Union, 2016).
14. A. Magnusson, " $^{14}\text{C}$  Produced by Nuclear Power Reactors - Generation and Characterization of Gaseous, Liquid and Solid Waste." PhD thesis, Lund University, Lund, Sweden (2007).
15. CAST, CAST (2018). <https://www.projectcast.eu>. Accessed 15 June 2022.
16. W. Kutschera, The half-life of  $^{14}\text{C}$ : Why is it so long? *Radiocarbon* **61**, 1135–1142 (2019).
17. K. Stenström, G. Skog, E. Georgiadou, J. Genberg, A. Mellström, "A guide to radiocarbon units and calculations" (Tech. Rep. LUNFD6[NFFR-3111]/1-17/[2011], Lund University, Lund, Sweden, 2011).
18. S. Szidat *et al.*,  $^{14}\text{C}$  analysis and sample preparation at the new Bern laboratory for the analysis of radiocarbon with AMS (LARA). *Radiocarbon* **56**, 561–566 (2014).
19. A. G. Hogg, L. K. Fifield, J. G. Palmer, C. S. M. Turney, R. Galbraith, Robust radiocarbon dating of wood samples by high-sensitivity liquid scintillation spectroscopy in the 50–70 kyr age range. *Radiocarbon* **49**, 379–391 (2007).
20. A. J. Fleisher, D. A. Long, Q. Liu, L. Gameson, J. T. Hodges, Optical measurement of radiocarbon below unity fraction modern by linear absorption spectroscopy. *J. Phys. Chem. Lett.* **8**, 4550–4556 (2017).
21. A. D. McCart, T. J. Ognibene, G. Bench, K. W. Turteltaub, Quantifying carbon-14 for biology using cavity ring-down spectroscopy. *Anal. Chem.* **88**, 8714–8719 (2016).
22. I. Galli *et al.*, Spectroscopic detection of radiocarbon dioxide at parts-per-quadrillion sensitivity. *Optica* **3**, 385–388 (2016).
23. "Council directive 2013/59/EURATOM laying down basic safety standards for protection against the dangers arising from exposure to ionising radiation" (Tech. Rep. 2013/59/EURATOM, European Council, European Union, 2013).
24. N. Toulhoat *et al.*, "Final report on results from work package 5: Carbon-14 in irradiated graphite (d5.19)" (Tech. Rep. D5.19, Project CAST, European Union, 2018).
25. M. Motta, Initial Activity of the ISPR-1 Reactor. *Ing. Nucleare*, pp. 3–12 (1961).
26. K. Abbas *et al.*, Development of an accelerator driven neutron activator for medical radioisotope production. *Nucl. Instrum. Methods Phys. Res. Sect. A* **601**, 223–228 (2009).
27. University of Cologne, Reached Precision (2021). <https://cologneams.uni-koeln.de/en/information-about-the-accelerator/ams-info/reached-precision>. Accessed 15 June 2022.
28. M. G. Delli Santi *et al.*, Biogenic fraction determination in fuel blends by laser-based  $^{14}\text{CO}_2$  detection. *Adv. Photon. Res.* **2**, 2000069 (2021).
29. I. Galli *et al.*, Optical detection of radiocarbon dioxide: First results and AMS intercomparison. *Radiocarbon* **55**, 213–223 (2013).
30. V. Remeikis *et al.*, Rapid analysis method for the determination of  $^{14}\text{C}$  specific activity in irradiated graphite. *PLoS One* **13**, e0191677 (2018).
31. European Commission, Research & Innovation Participant Portal (2020). <https://tiny.one/H36Cl>. Accessed 15 June 2022.
32. A. Bulgheroni, Complete set of spectroscopy result files from AMS/Scar experimentations. Joint Research Centre Data Catalogue. <https://data.jrc.ec.europa.eu/dataset/7002ce48-f46a-4d19-be3b-37f93852b586>. Accessed 28 June 2022.